Structural Characteristics of the Tallest Mangrove Forests of the American Continent: A Comparison of Ground-Based, Drone and Radar Measurements

Gustavo A. Castellanos-Galindo[1,2,3]*, Elisa Casella[3], Hector Tavera[4], Luis Alonso Zapata Padilla[1] and Marc Simard[5]

[1] WWF Colombia, Cali, Colombia, [2] Smithsonian Tropical Research Institute (STRI), Panama City, Panama, [3] Leibniz Centre for Tropical Marine Research (ZMT), Bremen, Germany, [4] Ministerio de Ambiente y Desarrollo Sostenible, Bogotá, Colombia, [5] Jet Propulsion Laboratory, California Institute of Technology, Pasadena, CA, United States

The Panama Bight eco-region along the Pacific coast of central and South America is considered to have one of the best-preserved mangrove ecosystems in the American continent. The regional climate, with rainfall easily reaching 5–8 m every year and weak wind conditions, contribute to the exceptionally tall mangroves along the southern Colombian and northern Ecuadorian Pacific coasts (Nariño Department and Esmeraldas Province areas). Here we evaluate the use of different methods (ground-based measurements, drone imagery and radar data [Shuttle Radar Topography mission-SRTM and TanDEM-X]) to characterize the structure of the tallest of these forests. In November 2019, three mangrove sites with canopy heights between 50 and 60 m, previously identified with SRTM data, were sampled close to the town of Guapi, Colombia. In addition to *in situ* field measurements of trees, we conducted airborne drone surveys in order to generate georeferenced orthomosaics and digital surface models (DSMs). We found that the extensive mangrove forests in this area of the Colombian Pacific are almost entirely composed of *Rhizophora* spp. trees. The tallest mangrove tree measured in the three plots was 57 m. With ca. 900 drone photographs, three orthomosaics (2 cm pixel^{-1} resolution) and digital surface models (3.5 cm pixel^{-1}) with average area of 4,0 ha were generated. The field-measured canopy heights were used to validate the drone-derived and radar-derived data, confirming these mangrove forests as the tallest in the Americas. The drone-derived orthomosaics showed significant patches of the Golden Leather Fern, *Acrostichum aureum*, an opportunistic species that can be associated to mangrove degradation, indicating that the mangrove forests investigated here may be threatened from increased selective logging requiring improvements and effective implementation of the current mangrove

management plans in Colombia. The techniques used here are highly complementary and may represent the three tiers for carbon reporting, whereby the drone-derived canopy height maps, calibrated with local *in situ* measurements, provides cheap but reliable Tier 3 estimates of carbon stocks at the project level.

INTRODUCTION

Spaceborne remote sensing (SRS) is nowadays a key tool to understand Earth phenomena including the monitoring of biodiversity on our planet (Pettorelli et al., 2016). This is the case for the use of SRS in monitoring mangrove ecosystems. Accelerating since 2000 and facilitated by the free availability of satellite products, different global datasets of mangrove cover and loss are now available (Worthington et al., 2020). These baseline products (e.g., Giri et al., 2011; Bunting et al., 2018) have helped to derive global datasets of important properties of mangrove such as above-ground biomass (AGB) and carbon (AGC) after extrapolating or averaging site-specific values (Rovai et al., 2016; Rovai et al., 2018; Hamilton and Friess, 2018). Other SRS products like Lidar and interferometric synthetic aperture radar (InSAR) have been recently used to estimate mangrove heights at national, regional and global scales greatly improving previous AGB estimates (Fatoyinbo and Simard, 2013; Shapiro et al., 2015; Lagomasino et al., 2019; Simard et al., 2019). Nevertheless, there are still limitations faced when using some of these SRS global products with respect to their resolution (usually > 25 m per pixel) and the climatic conditions under which images can be taken (e.g., cloud free conditions).

Ideally, local and national mangrove mapping datasets that use remote sensing products with higher resolutions and that incorporate ground-truth measurements can play an important role in providing training data and validation for many of the on-going global mapping exercises (e.g., Global Mangrove Watch initiative; Worthington et al., 2020). Hence coordination and integration of global, national, and local datasets are needed to overcome many of the limitations of individual datasets.

Consumer-grade drones, belonging to the unoccupied aircraft systems (UAS) sector, appear to be an appropriate tool to overcome some of the limitations of SRS products in mangrove areas that are < 100 ha (Castellanos-Galindo et al., 2019). Examples of mapping mangrove forest with drones at spatial resolutions with centimeter scale are rapidly appearing in the literature (Otero et al., 2018; Li et al., 2019; Navarro et al., 2020). These finer resolution products provide unique opportunities to understand ecological processes and derive essential biodiversity variables that would not be possible to obtain with SRS at the moment. The use of UAS in mangrove mapping is therefore likely to simplify and complement traditional field inventories and additionally increase the accuracy of AGB and AGC estimates at the local level (e.g., Lucas et al., 2020). Collecting drone-derived information can therefore greatly benefit the calibration of the regional and global estimates that have been produced so far using SRS products of coarser resolution.

The Panama Bight eco-region in the west coast of Central and South America is considered to have one of the best-preserved mangrove ecosystems in the American continent and is thus a widely recognized conservation hotspot (Spalding et al., 2007). Highly developed mangrove forests are found along the southern Colombian and northern Ecuadorian Pacific coasts (Nariño and Esmeraldas areas; Castellanos-Galindo et al., 2015; Hamilton et al., 2017). Already in the mid-twentieth century, the American Geographer Robert West referred to these intertidal forests as the "most luxuriant mangroves of the world" (West, 1956). A more recent study (Simard et al., 2019) has identified the southern Colombian Pacific coast (Cauca and Nariño Departments), together with Gabon and Equatorial Guinea in Africa, as the regions containing the tallest mangroves in the world. A combination of high precipitation (i.e., potentially lower salinity), high temperature and low cyclone landfall frequency plus local geomorphological factors are associated to the observed exceptionally large areas and high canopy heights observed in those regions (Simard et al., 2019).

Mangroves in the southern Colombian Pacific coast occur in areas with geomorphological features like alluvial plains that form dynamic barrier islands surrounded by tidal channels (Martínez et al., 1995). These mangroves may be the wettest in the world with rainfall easily reaching 5 to ca. 8 m every year. The remoteness of this vast area (with no coastal road and only accessible by long boat journeys or small airplanes) contributes to the relatively pristine nature of some of these forests, but also to the difficulty in obtaining scientific ecological information (Castellanos-Galindo et al., 2021). This difficulty has prevented so far corroborating most of the information from modeling studies that have highlighted the unique characteristics of the mangrove areas in this coast (e.g., Hutchison et al., 2014; Rovai et al., 2018).

To validate previous remote sensed measurements (i.e., Simard et al., 2019) and to assess the complementarity of different techniques, we compare here mangrove tree height and AGB measurements from ground-based inventories, drone imagery and radar data (from the Shuttle Radar Topography mission-SRTM and the TerraSAR-X add-on for Digital Elevation Measurement-TanDEM-X) taken from a remote area in the Colombian Pacific coast recognized to contain the tallest mangroves in the American continent. The combination of field-based methods (tree DBH and height measurements and drone photogrammetry) with existing SRS products in the most extreme range of mangrove canopy height (∼50 m) allows for the first time: (1) the validation of previous models that highlighted the ecological value of mangroves in this region and (2) the recognition that these areas are in need of urgent protection due on-going localized alterations.

MATERIALS AND METHODS

Study Site

The Colombian Pacific coast encompasses ca. 1,500 km in the tropical eastern Pacific biogeographic region that extends from the Gulf of California, Mexico to northern Peru. Almost 2/3 of this coastal region is dominated by mangroves, with ~80% of the total mangrove area of Colombia (Mejía-Rentería et al., 2018). The whole coast presents annual precipitations of > 2,000 mm, reaching in some areas 8,000 mm yr^{-1}. This extreme precipitation translates into year-long low water salinities (<30) and permanent brackish areas inside bays, small deltas and tidal channels in what is identified as the Eastern Pacific fresh pool (Alory et al., 2012). The tidal regime is semi-diurnal, meso- to macro-tidal with amplitudes during spring tides greater than 4 m (Correa and Morton, 2010). These tidal conditions indicate that mangroves and mudflats are completely exposed at low tides and completely inundated at high tide (during both neap and spring tides).

Nariño, the southernmost coastal Department along the Pacific coast of Colombia, borders the neighboring Esmeraldas province of Ecuador to the South, and the Colombian Cauca Department in Colombia to the North. Nariño alone contains 46% of the total mangrove forests of the country (Mejía-Rentería et al., 2018). This tectonically active coast is characterized by the presence of two high water discharge and dynamic deltas (Mira and Patía; Restrepo and Cantera, 2013) and an almost uninterrupted mangrove belt. The coast is also under-developed in terms of infrastructure with the presence of small villages (<5,000 inhabitants) scattered in a mangrove-dominated landscape. Nariño contains the largest mangrove marine protected area (MPA) of the whole tropical eastern Pacific (the Sanquianga National Park with ~80,000 ha) and a more recently created mangrove MPA bordering Ecuador (Distrito Nacional de Manejo Integrado Cabo Manglares Bajo Mira y Frontera). North of Sanquianga MPA lies the mouth of the Iscuandé River, an estuarine area dominated by extensive mangrove forests and small human settlements that constitute the Afro-Colombian community council of Esfuerzo Pescador. The water discharge of the Iscuandé River is 6.71 km^3 yr^{-1} (Restrepo and Kjerfve, 2004).

Field Sampling

In November 2019 (6th–8th), three different mangrove sites in the northern coast of the Nariño Department of the Colombian Pacific coast were visited (**Figure 1**). The sites are located near the mouth of the Iscuandé River, an estuarine area completely dominated by mangrove forests, tidal creeks and mud-sand flats that emerge during low tides. Circular plots of 15 m-diameter were established at each site. Ground measurements within these plots included the identification of tree species, diameter at breast height (DBH) and top height of selected trees. While DBH measurements were generally made around the trunk of each tree at 1.3 m above the ground surface, several measurements were made above the high prop roots of *Rhizophora* spp. (e.g., **Figure 2**). To measure DBH, a diameter tape was wrapped around

the girth of each tree and a diameter measurement read was made to the nearest 0.1 cm. Heights of selected trees within each plot were collected with the aid of a Nikon Forestry Pro II laser hypsometer. There trees were then geolocated using a handheld GPS (Bad Elf GNSS Surveyor).

Allometric Equations

For each of the plots surveyed, we used the DBH values and two allometric equations to determine tree biomass per hectare. First, we used the allometric equation for *Rhizophora mangle* developed by Fromard et al. (1998) to estimate tree biomass that only takes into account DBH:

$$AGB = 0.1282 \times D^{(2.6)}$$

We also used the pantropical tree allometric model to estimate AGB proposed by Chave et al. (2014) which takes into account tree height, DBH and wood specific gravity:

$$AGB_{est} = 0.0673 \times \left(\rho D^2 H \right)^{0.976}$$

where D is DBH in cm, H is tree height in m and ρ is wood specific gravity in g cm^{-3}. ρ was computed as the mean value of the wood specific gravity values available for *Rhizophora* spp. in the Central and South America from the Global wood density database (Chave et al., 2009; Zanne et al., 2009).

To implement the pantropical tree allometric model of Chave et al. (2014), we back-calculated the heights of the trees for which we only had DBH. For that we fitted, a Log-Log model of DBH:H with 26 trees for which we had both DBH and Heights (see **Supplementary Figure 1**). Total living carbon was then calculated using the relationship total living biomass:living carbon of 1:0.464 (Kauffman et al., 2011, 2020).

Drone Surveys

Drone surveys in the direct vicinity of each plot were carried out at low tide with calm winds. The drone patches surveyed were ~3 ha in size at each site and always covered the plot areas where ground measurements were taken. Low-altitude (100 m) aerial images were acquired using two UAS, DJI Mavic Pro and Mavic 2 Pro. These drones are equipped with integrated photo cameras. DJI Mavic Pro has a FC220 camera, with a sensor 1/2.3" CMOS (effective pixel:12,35 Megapixel), focal length of 5 mm, a pixel size of 1.7 × 1.7 μm and a resolution of 4,000 × 2,250 pixels. The Mavic 2 Pro has a L1D-20c camera with a sensor 1" CMOS camera (effective pixel:20 Megapixel), focal length of 10 mm, a pixel size of 2.41 × 2.41 μm and a resolution of 5,472 × 3,648 pixels. Photos are geotagged by the DJI integrated GPS/GLONASS location system with a horizontal and vertical precision of up to ± 1.5 and ± 0.5 m, respectively.[1] Flights were performed in automated mode and were programmed using the commercial web app "Drone Deploy." Due to the nature of the environment, characterized by dense vegetation with lack of large gaps exposing the terrain within the forest, it was not possible to easily place and collect ground control points (GCPs). Although few small gaps are present, they are not easily accessible and lack

---

[1] www.dji.com/mavic
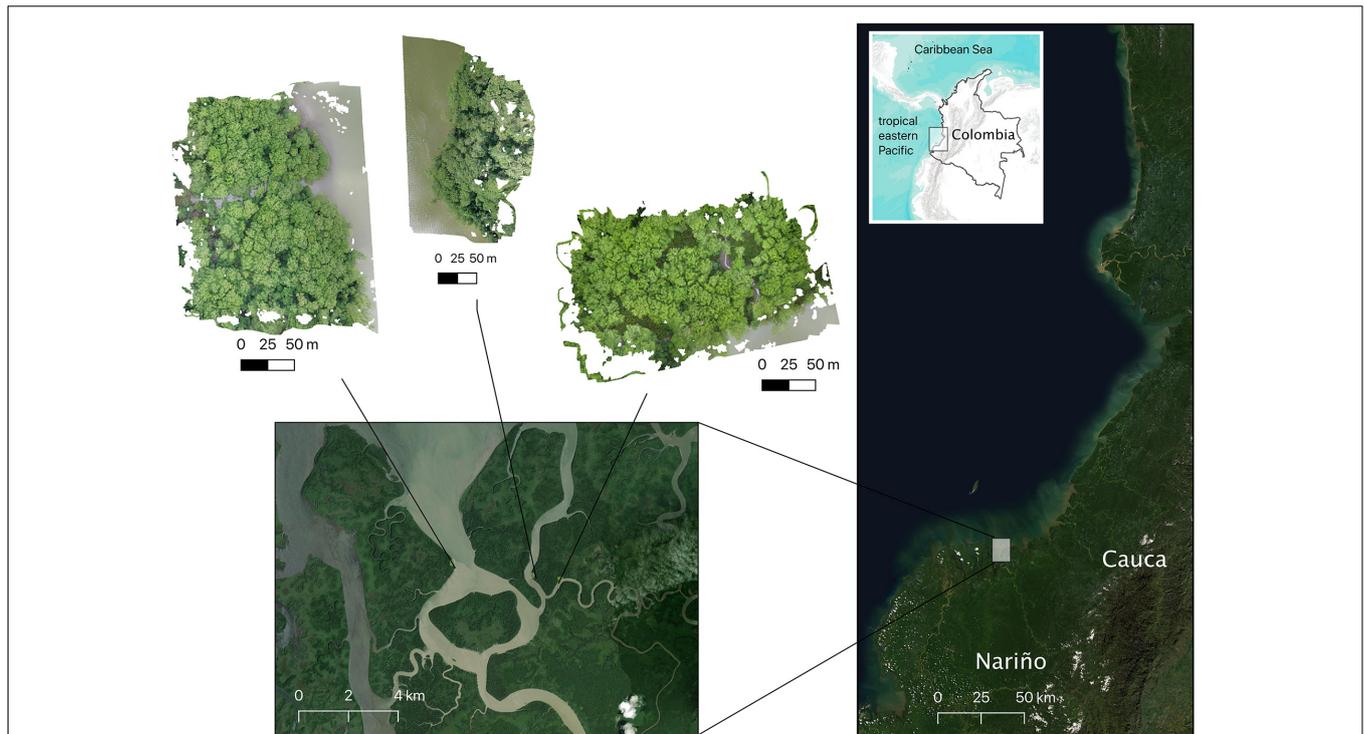
FIGURE 1 | Location of the mangrove sites visited in the southern Colombian Pacific coast (Iscuandé River mouth, Nariño Department; Imagery ©2021 Google, Maxar Technologies, Data SIO, NOAA, U.S. Navy, NGA, GEBCO, Landsat/Copernicus, Imagery ©2021 Terrametrics, Map data ©2021). Three mangrove patches were surveyed in the estuarine complex formed close to the mouth of the Iscuandé River: from left to right, sites are known as: "La Punta del Codo," "La Rotura," and "Madrid."
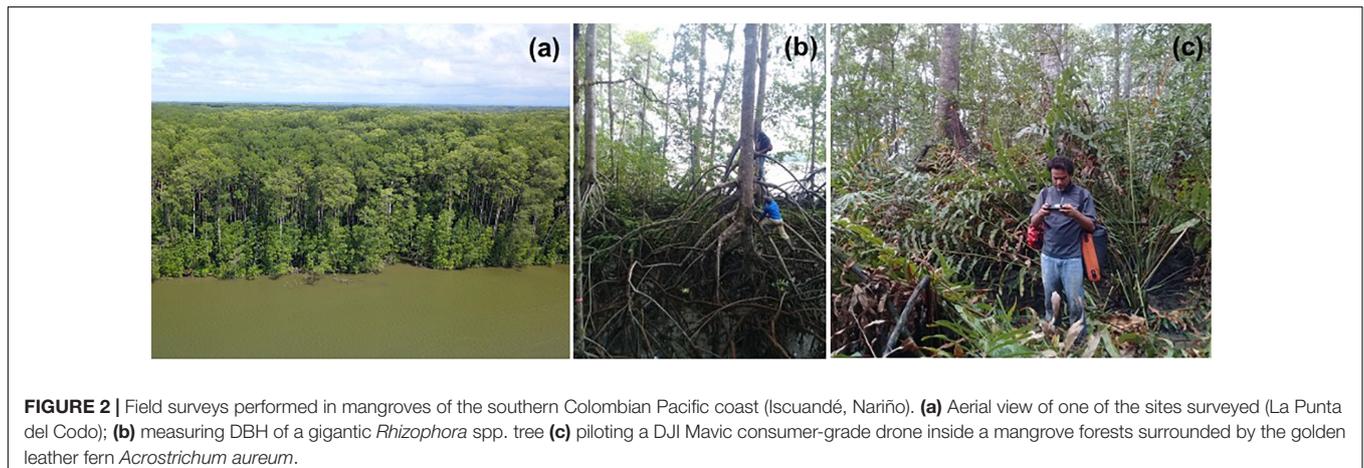
FIGURE 2 | Field surveys performed in mangroves of the southern Colombian Pacific coast (Iscuandé, Nariño). **(a)** Aerial view of one of the sites surveyed (La Punta del Codo); **(b)** measuring DBH of a gigantic *Rhizophora* spp. tree **(c)** piloting a DJI Mavic consumer-grade drone inside a mangrove forests surrounded by the golden leather fern *Acrostrichum aureum*.

the necessary sky view to operate GNSS and collect GCPs with acceptable accuracy.

The acquired images were analyzed and processed using the software Agisoft Metashape.[2] Metashape is based on Structure from Motion (SfM) (Ullman, 1979) and Multi-View Stereo reconstruction (MVS) methods (Scharstein and Szeliski, 2002; Seitz et al., 2006). For a comprehensive description of the SfM method implemented in Metashape, the reader

is referred to Westoby et al. (2012). Metashape gives as outputs an orthorectified photomosaic (orthomosaic) and a Digital Surface Model (DSM) from nadir photos collected during the flight. The output models were georeferenced in Metashape to the WGS84 datum using camera positions. The results of the photogrammetric suite were used in the three locations to estimate different environmental variables. Orthomosaics with 2 cm/pixel resolution allowed detecting the heterogeneity of vegetation and the presence of opportunistic species associated to mangrove degradation. DSMs were

---

[2]www.agisoft.com

used to estimate the heights of trees within the *in situ* sampling areas. Since the ground was not visible within the forest, we used the elevation of mud-sand flats that emerge during low tides as a reference. The observed DSM was vertically shifted to match the elevation of the mud-sand flats. Consequently, the height of the trees was extracted from the vertically shifted DSM.

Satellite Data

To compare our *in situ* and drone generated data, we used two global RS products generated by Simard et al. (2019). One of maximum mangrove canopy height for the year 2000 with a resolution of ∼30 m that used the Shuttle Radar Topography Mission (SRTM) global digital elevation model (DEM), and the Geoscience Laser Altimeter System (GLAS) global Lidar altimetry products. The second RS product was an aboveground mangrove biomass map that was generated by Simard et al. (2019) linking field-measured biomass–height allometry with SRTM estimates of basal area weighted height (all RS products available at https://daac.ornl.gov/cgi-bin/dsviewer.pl?ds_id=1665).

We additionally compared our mangrove height field-generated data against the high-resolution data product (12 × 12 m) derived from the TerraSAR-X add-on for Digital Elevation Measurement-TanDEM-X mission (Simard unpublished *data*). We performed a similar procedure as with the drone DSMs and adjusted the TanDEM-X DEM shifting it vertically to match the elevation of the adjacent water. For details about use of the TanDEM-X in mangrove canopy height estimations see Lee and Fatoyinbo (2015) and Lagomasino et al. (2016).

The tree height comparisons between the three methods used was done using the ground height measurements taken at the three sites surveyed (n = 21 trees). With the georeferenced location of each of these trees, a vector (∼5 m radius circle) was created in QGIS and using the zonal statistics, height information (mean, maximum and minimum) from the drone, the SRTM and the TanDEM-X rasters were extracted. We fitted linear regressions between *in situ* maximum tree heights and calculated drone, SRTM and TanDEM-X tree heights. In addition, Pearson,

determination coefficients and RMSE (root mean squared error) were computed to assess the fit of the regressions.

RESULTS

All surveyed sites were dominated by the red mangrove *Rhizophora* spp. In one of the sites (Madrid; **Figure 3**), the golden leather fern *Acrostrichum aureum*, a mangrove associate, dominated the understory which in many cases reached up to 4 m (see **Figures 2**, **4**). While still difficult to distinguish in the drone orthomosaic, we estimated that at least 5% of the orthomosaic obtained for the Madrid site was completely covereded by *A. aurem* (i.e., gaps with no *Rhizophora* spp. canopies). Moreover, our ground surveys at this site showed that the understory in the remaining 95% of the orthomosaic was completely dominated by this species, which was not captured by the drone orthomosaic (**Figure 4**).

Mean DBH values were very high at the Madrid site in comparison with the other two surveyed sites. The Madrid site was characterized by the largest trees with a mean DBH of 52.4 cm reaching a DBH and height of 96.7 cm and 57 m, respectively. In contrast, the mean DBH at La Rotura and La Punta del Codo sites, were considerably lower (around 20 cm) with maximum tree heights of 50.8 and 53.6 m, respectively. The low mean DBH values indicate the presence of comparatively smaller trees in those two latter sites. Nonetheless, the total AGB was, as expected, dominated by the presence of the largest trees in all sites. Depending on the allometric equation used (Fromard et al., 1998; Chave et al., 2014), the mean AGB across all sites was 862.2 or 626.4 Mg ha^{-1}, respectively. Similarly, mean above-ground mangrove carbon stocks were estimated in 400.1 or 290.7 Mg C ha^{-1} (**Table 1**). These values, especially in the Madrid site do not account for the contribution of *A. aurem* to the total biomass and carbon. The mangrove AGB values derived from the ground data were two to three times higher than those estimated with the SRTM data in Simard et al. (2019). AGB values for the examined plots derived from SRTM, and based on continental scale allometry, ranged from 296.2 to 413.3 to Mg ha^{-1}.

FIGURE 3 | The three RGB orthomosaics obtained with the drone data showing the geo-referenced location of the trees measured for height using the Nikon Forestry Pro II laser hypsometer.
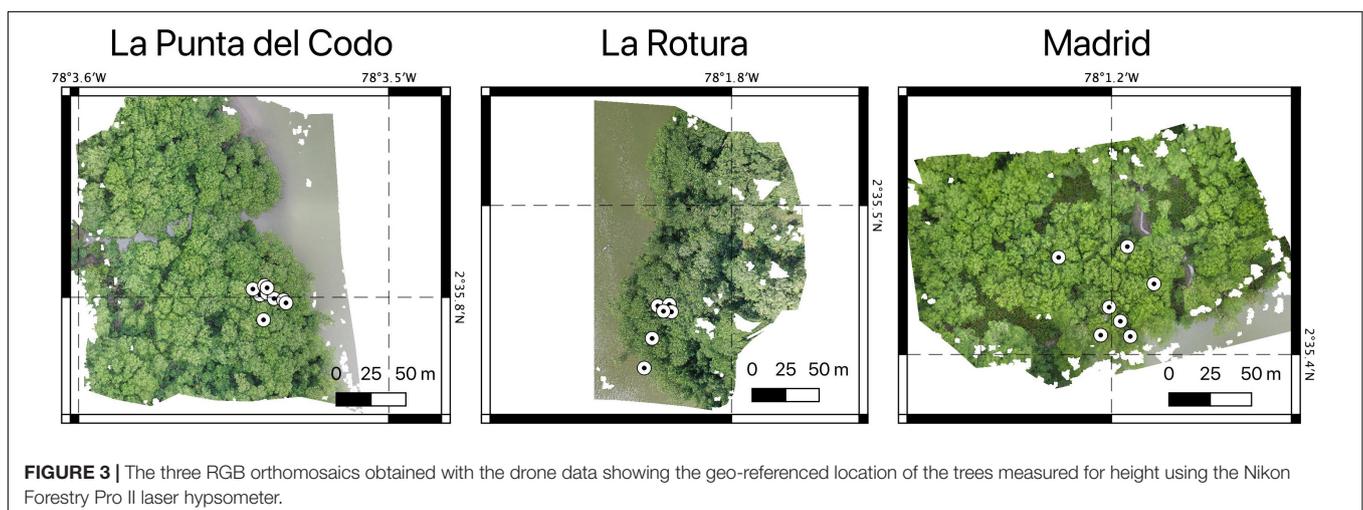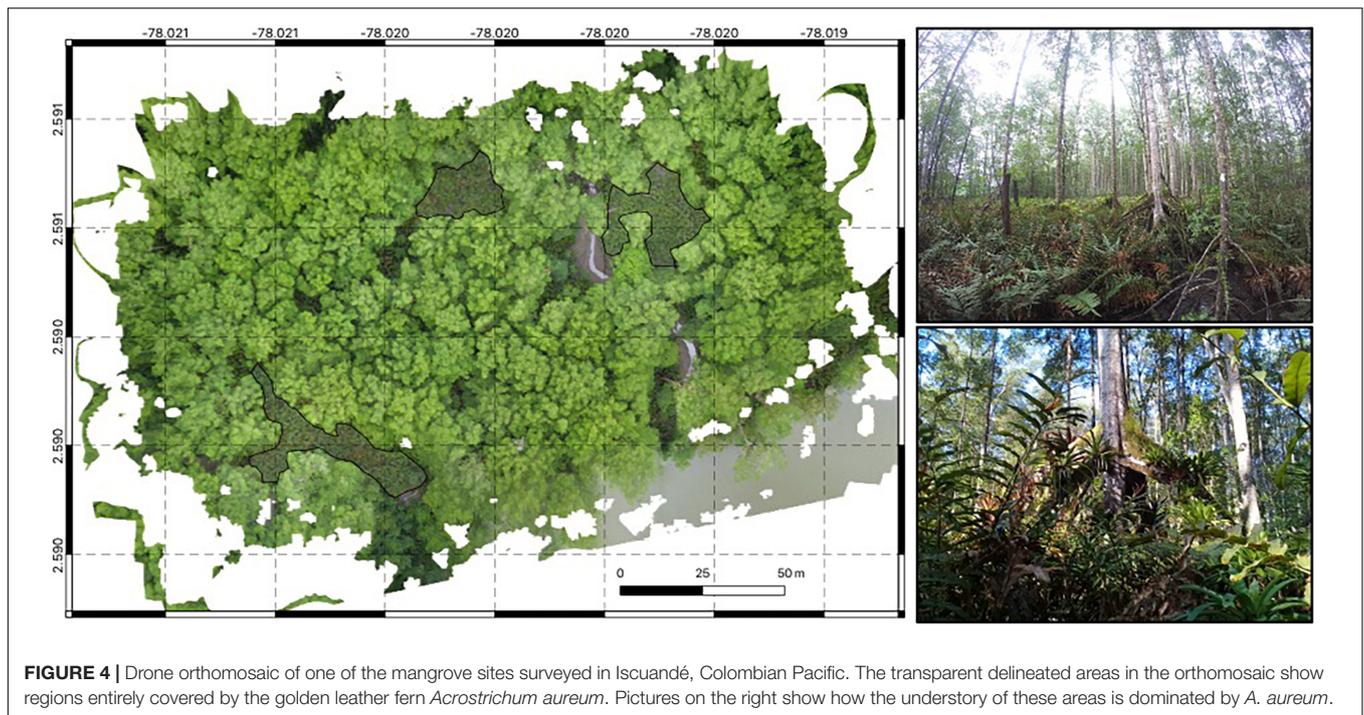
FIGURE 4 | Drone orthomosaic of one of the mangrove sites surveyed in Iscuandé, Colombian Pacific. The transparent delineated areas in the orthomosaic show regions entirely covered by the golden leather fern *Acrostichum aureum*. Pictures on the right show how the understory of these areas is dominated by *A. aureum*.

TABLE 1 | Summary statistics for the field measurements (diameter at breast height-DBH, maximum height, basal area, and tree density) taken at three mangrove sites in Iscuandé, Colombian Pacific coast.

Site	Samples (n)	Mean DBH (cm)	Max DBH (cm)	Min DBH (cm)	Mean tree height (m)	Max tree height (m)	Basal area (m² ha⁻¹)	Tree density (trees ha⁻¹)	Chave et al. (2014) Pantropical equation		Fromard et al. (1998) Equation	
									AGB (Mg ha⁻¹)	C storage (Mg ha⁻¹)	AGB (Mg ha⁻¹)	C storage (Mg ha⁻¹)
La Punta del Codo	27	22.7	73.9	5.0	47.0	53.6	28.4	382.0	848.0	393.5	579.4	268.8
La Rotura	33	19.5	92.0	5.0	46.1	50.8	33.4	466.9	902.1	418.6	667.6	309.8
Madrid	22	52.4	96.7	14.1	47.2	56.7	30.1	114.3	836.4	388.1	632.3	293.4

DISCUSSION

We conducted a field campaign specifically to validate and study the regions with the tallest mangrove forests in the Americas (Simard et al., 2019). Field measurements of tree DBH and height were used to validate drone- and SRTM- derived maps of mangrove canopy height, confirming the findings of Simard et al. (2019). The tallest field-measured tree was 57 m, the drone-derived canopy height revealed maximum heights of 57.6 m and the SRTM data for these sites showed maximum canopy heights of 54.3 m. While our analysis is performed in forest stands that may not be representative of the entire region, we show that *in situ*, drone and spaceborne data provide accurate results in the most extreme range of mangrove canopy height. All the three data sources corroborate the existence of exceptionally tall mangrove forests in this region of the Western American tropics. However, each of the methods used to estimate tree height data presented challenges and associated errors (**Figure 5** and **Table 2**). As revealed in previous modeling studies (e.g.,

Rovai et al., 2016; Hamilton and Friess, 2018; Rovai et al., 2018), *in situ* measurements confirmed that these sites are on the upper range of mangrove biomass and carbon per area in the world.

Field tree height data was collected with a laser range finder (Nikon Forestry Pro II laser hypsometer). In a recent study, Saliu et al. (2021) indicated that this method presents the lowest amount of error (8%) among a variety of methods used to measure mangrove tree heights in Malaysia. Larjavaara and Muller-Landau (2013) have also identified that both methods (tangent and sine) available when using the laser range finder can incur in high random errors and underestimations in moist tropical forests. A few aspects complicate mangrove tree height calculations with this instrument. For example, in highly dense forests, the identification of the ground and the top of the tree crown can be challenging and thus is not exempt from errors. For a mangrove system in the Colombian Caribbean, Simard et al. (2008) calculated that the random error of tree height measurements in the field can be ~10%. In the forests examined
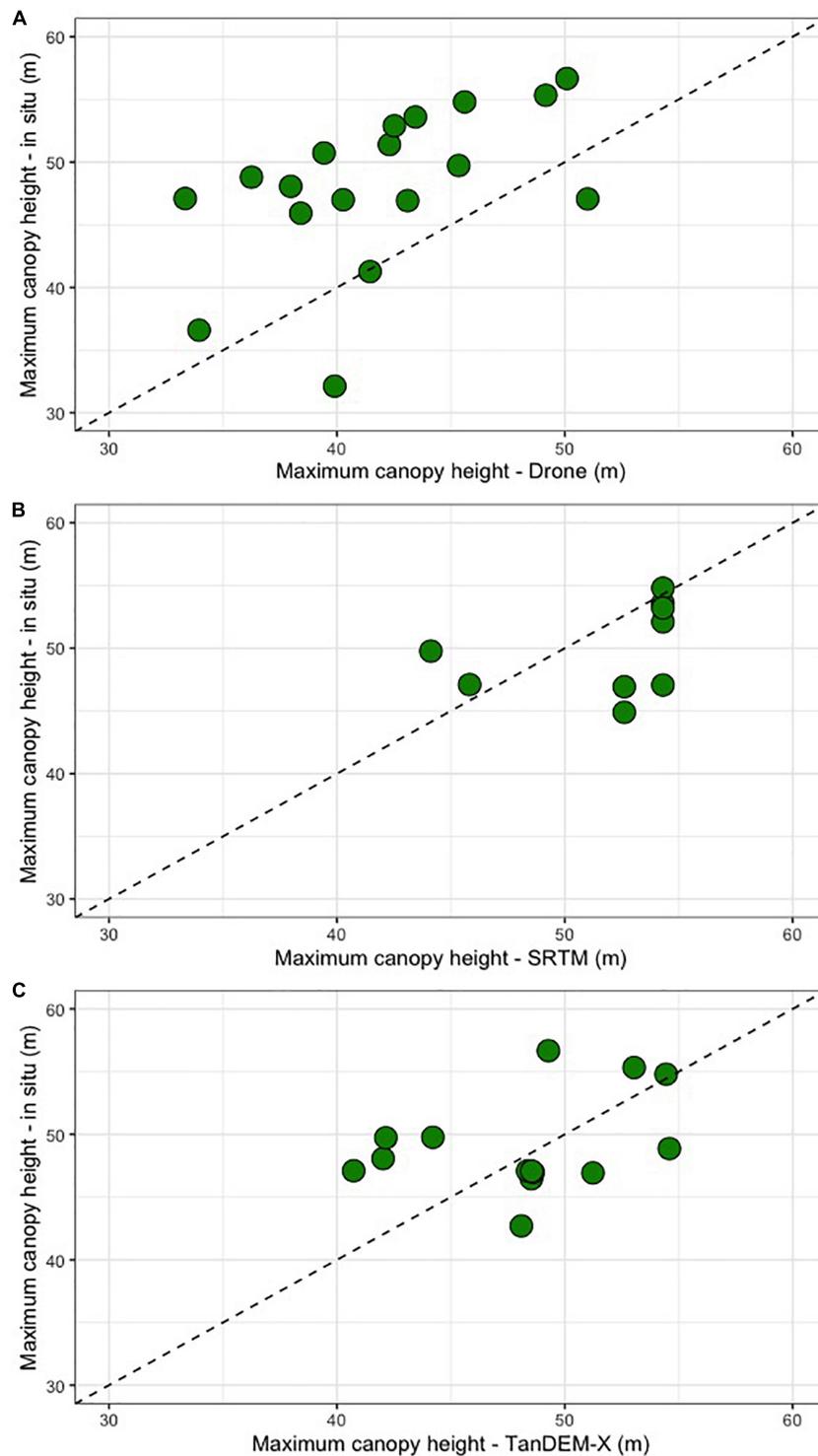
FIGURE 5 | Correlation between different methods to calculate mangrove tree heights in three different sites in Iscuandé, Colombian Pacific. **(A)** Scatter plot of *in situ* Height$_{max}$ vs. Drone Height$_{max}$; **(B)** scatter plot of *in situ* Height$_{max}$ vs. SRTM Height$_{max}$; **(C)** scatter plot of *in situ* Height$_{max}$ vs. TanDEM-X Height$_{max}$.

here, the presence of a dense understory in some sites plus the stilt root nature of *Rhizophora* trees also complicate the identification of the ground with the laser range finder. While we consider these *in situ* measurements to be the most reliable estimates of tree height, we acknowledge the potentially significant uncertainty associated with this method.

Summary statistics showing results of linear regressions and Pearson correlations for the comparison among the three different tree height measurements.

Methods compared	Pearson coefficient (*r*)	Determination coefficient (*R²*)	RMSE (m)
In situ vs. drone	0.25	0.06	5.69
In situ vs. SRTM	0.34	0.12	3.18
In situ vs. TanDEM-X	0.34	0.12	3.55

Mangrove Above-Ground Biomass of the Iscuandé Region in the Global Context

The mean mangrove AGB values obtained here using the *in-situ* data are extremely high varying between 862.2 and 626.4 Mg ha^{-1} (depending on which allometric equation is used). These values are located in the upper range of the recent global synthesis by Rovai et al. (2021) and also correspond to the upper range values recently estimated by Trettin et al. (2021) for a mangrove forest in Gabon where mangrove trees of up to 60 m can be found. Our estimated mean AGB values are generally higher than those obtained using the AGB values calculated by Simard et al. (2019) for the same areas. This result warrants a re-examination of the relationship between SRTM data and *in situ* inventories considering a larger dataset than the one currently considered in our study. Likewise, it is important to consider that our plots represent very tall mangrove forests within the Iscuandé area. A more representative AGB (and carbon) estimate would need a sampling design that considers the whole range of mangrove type mosaics and patch heterogeneity that are present in this large area (e.g., like the recent work of Trettin et al., 2021 in Gabon). Such a study could yield slightly lower mean AGB values for these mangrove forests but would also contribute to more accurate numbers on carbon stocks of these areas.

Advantages of Drone-Derived Data to Detect Mangrove Degradation

The drone derived data (orthomosaics and DSMs) of these three mangrove sites provided sufficiently detailed information (<4 cm pixel^{-1} resolution) to detect landscape features that are not captured with the ground surveys nor with the SRTM or the TanDEM-X products. Especially important are (1) the heterogeneity in canopy heights observed and also (2) the detection of canopy gaps that are the result of possible deforestation (i.e., selective logging). On one hand, the drone-derived DSMs (3.5 cm pixel^{-1} resolution) recorded highly variable tree heights within each of the 3 ha patches. On the

FIGURE 6 | Comparison of altimetry products derived from surveys in mangroves of Iscuandé (Colombian Pacific coast). Mangrove patches correspond to "La Punta del Codo," "La Rotura" and "Madrid" from left to right. The upper row shows the vertically shifted DSMs obtained from the drone data. The middle row depicts canopy heights from the TanDEM-X product (Simard unpublished; © DLR 2020) The lower row corresponds to canopy heights from the Simard et al. (2019) dataset.

other hand, the pixels SRTM and TanDEM-X products may include tree crowns of short and tall trees or ground areas, thus these elevation of these mixed pixels represent overall canopy height rather than the height of the tallest tree. This effect may be particularly important in this study (**Figure 6**), with tree heights measured near forest edges along the shore or around canopy gaps.

On the other hand, the drone orthomosaics were sufficiently detailed to detect the presence of gaps within one of the mangrove patches that were dominated by the golden leather fern *A. aureum*, an opportunistic species associated to mangrove degradation (Madrid patch in **Figure 4**). *Acrostichum aureum* is a highly resistant fern able to colonize the understory of mangrove areas when facilitated either by the presence of natural canopy gaps (see Amir, 2012; Amir and Duke, 2019) or by man-made gaps produced after forest logging. The fern is commonly associated to deforestation and is able to rapidly colonize mangrove areas that have been disturbed, a process that has been defined as cryptic (mangrove) ecological degradation (Dahdouh-Guebas et al., 2005; Blanco et al., 2012). Once established, *A. aureum* modifies the geomorphology and hydrology, impeding natural regeneration and hindering animal movement (Medina et al., 1990; Biswas et al., 2018). Other aspects of the effects of this fern on ecosystem processes within the mangrove forests are poorly understood. The information provided by the drone products on *A. aureum* can be valuable as it provides evidence at the scale of 10 s of hectares on loss of mangrove ecosystem health that would otherwise be unnoticed when using coarser SRS products. These highly detailed drone products can also aid in the development of complexity indexes, such as those proposed in Blanco et al. (2001), that could be used to characterize health status and degradation in mangrove forests. Being able to identify the understory vegetation (e.g., *A. aureum* in this case) of a mangrove area with the drone products implies also that the contribution of this vegetation to the ecosystem biomass and carbon storage, which could become very high, could be accounted for. However, it is unclear how persistent in time *A. aureum* can become in this region. Surprisingly, allometric equations and information on the carbon content and establishment dynamics of this opportunistic fern are scarce and needed.

The mangrove areas examined here, still contain well developed forests. However, historical mangrove timber exploitation has occurred and continues to occur. Although we do not have data on the magnitude of recent and on-going logging, the local communities identify this activity as an increasingly pressing factor on the surrounding mangrove ecosystems. Moreover, unaccounted as a mangrove degradation source remains the effects that the anti-narcotics national program for eradication of coca crops that the Colombian government undertook in the 2000s with aerial aspersion of glyphosate (and currently seeks to continue). One of the few accounts on the use of herbicides in mangrove forests is that of the severe effects that its use caused on Vietnam forests during the second Indochina war (Westing, 1983). Anecdotal information from locals in Iscuandé reported on the effects that glyphosate had on native flora and fauna around mangroves in the past. The

localized effects that both timber logging and glyphosate could have on these exceptionally well-developed mangroves could be studied with the finer resolution products from drones.

Implications for Mangrove Carbon Monitoring in Remote Areas

Our study reveals significant challenges in collecting field and drone data in these mangrove areas. These can be categorized as logistical and geometrical. The access to these sites requires careful travel planning that includes site accessibility by plane and boat in a highly dynamic setting driven by the large tidal range, and close collaboration with local authorities and organizations. The latter facilitates, not only safe passage to sites, but gathering of a wealth of knowledge about local landscapes, cultural practices and customs related to mangroves and water management (see Oslender, 2016). On the other hand, the geometrical challenges are related to the complex terrain with mangroves roots, litter, and mud that constrains the possibility to collect tree heights in a systematic and time-efficient way. To accurately process the drone data, collecting ground control points-GCPs (ideally with a Real-time kinematic-RTK GPS) is desirable. However, identifying sufficiently clear gaps to place those GCPs inside mangrove forests can prove an unachievable task. Ways to overcome this limitation could include using drones that have incorporated an RTK GPS (although this technique does not completely exclude the need of GCPs) and/or using adjacent ecosystems within the mangrove forest (e.g., mudflats) where placing GCPs is feasible.

Zeng et al. (2021) suggests that mangrove blue carbon projects in Colombia may only be profitable in the southern Colombian Pacific coast, the area where this study was conducted. Our results, therefore provide valuable assessment methodologies and an initial *in situ* assessment of carbon stocks for potential blue carbon projects in an area that has been highlighted by modeling studies as a blue carbon hotspot in the world with much need of effective conservation actions. The techniques are complementary and may represent the three tiers for carbon reporting, whereby the drone-derived canopy height maps, calibrated with local *in situ* measurements, provides affordable and reliable Tier 3 estimates of carbon stocks at the project level. These detailed estimates can in turn help calibrating the coarser Tier 1 and Tier 2 assessments. Additionally, the combination of drone and ground survey data can provide a way to detect and monitor small-scale ecosystem degradation symptoms that so far are not possible to detect with the SRS products currently used for mangrove mapping. This can bring a more detailed understanding of landscape processes occurring within these vulnerable ecosystems that so far have been excessively focused on coarse area measurements.

DATA AVAILABILITY STATEMENT

The original contributions presented in the study are included in the article/**Supplementary Material**, further inquiries can be directed to the corresponding author/s.

SUPPLEMENTARY MATERIAL

The Supplementary Material for this article can be found online at: https://www.frontiersin.org/articles/10.3389/ffgc.2021.732468/full#supplementary-material

Raw forest inventory data are also available at https://doi.org/10.6084/m9.figshare.16509045.v2.

REFERENCES

Alory, G., Maes, C., Delcroix, T., Reul, N., and Illig, S. (2012). Seasonal dynamics of sea surface salinity off panama: The far Eastern Pacific Fresh Pool. *J. Geophys. Res* 117:C04028. doi: 10.1029/2011JC007802

Amir, A. A. (2012). Canopy gaps and the natural regeneration of Matang mangroves. *For. Ecol. Manag.* 269, 60–67. doi: 10.1016/j.foreco.2011.12.040

Amir, A. A., and Duke, N. C. (2019). Distinct characteristics of canopy gaps in the subtropical mangroves of Moreton Bay. *Australia. Estuar. Coast. Shelf Sci.* 222, 66–80. doi: 10.1016/j.ecss.2019.04.007

Biswas, S. R., Biswas, P. L., Limon, S. H., Yan, E. R., Xu, M. S., and Khan, M. S. I. (2018). Plant invasion in mangrove forests worldwide. *For. Ecol. Manag.* 429, 480–492. doi: 10.1016/j.foreco.2018.07.046

Blanco, J. F., Bejarano, A. C., Lasso, J., and Cantera, J. R. (2001). A new look at computation of the complexity index in mangroves: do disturbed forests have clues to analyze canopy height patchiness? *Wetl. Ecol. Manag.* 9, 91–101. doi: 10.1023/A:1011115220126

Blanco, J. F., Estrada, E. A., Ortiz, L. F., and Urrego, L. E. (2012). Ecosystem-wide impacts of deforestation in mangroves: the Urabá Gulf (Colombian Caribbean) case study. *Int. Sch. Res. Not.* 2012, 1–14. doi: 10.5402/2012/958709

Bunting, P., Rosenqvist, A., Lucas, R., Rebelo, L.-M., Hilarides, L., Thomas, N., et al. (2018). The global mangrove watch—a new 2010 global baseline of mangrove extent. *Remote Sensing* 10:1669. doi: 10.3390/rs10101669

Castellanos-Galindo, G. A., Cantera, J. R., Saint-Paul, U., and Ferrol-Schulte, D. (2015). Threats to mangrove social-ecological systems in the most luxuriant coastal forests of the Neotropics. *Biodivers. Conserv.* 24, 701–704. doi: 10.1007/s10531-014-0827-y

Castellanos-Galindo, G. A., Casella, E., Mejía-Rentería, J. C., and Rovere, A. (2019). Habitat mapping of remote coasts: evaluating the usefulness of lightweight unmanned aerial vehicles for conservation and monitoring. *Biol. Conserv.* 239:108282. doi: 10.1016/j.biocon.2019.108282

Castellanos-Galindo, G. A., Kluger, L. C., Camargo, M. A., Cantera, J., Mancera Pineda, J. E., Blanco-Libreros, J. F., et al. (2021). Mangrove research in Colombia: temporal trends, geographical coverage and research gaps. *Estuar. Coast. Shelf Sci.* 248:106799. doi: 10.1016/j.ecss.2020.106799

Chave, J., Coomes, D., Jansen, S., Lewis, S. L., and Swenson, N. G. (2009). Towards a worldwide wood economics spectrum. *Ecol. Lett.* 12, 351–366. doi: 10.1111/j.1461-0248.2009.01285.x

Chave, J., Réjou-Méchain, M., Burquez, A., and Chidumayo, E. (2014). Improved allometric models to estimate the aboveground biomass of tropical trees. *Glob. Chang. Biol.* 20, 3177–3190.

Correa, I., and Morton, R. (2010). "Pacific coast of Colombia," in *Encyclopedia of the world's coastal landforms*, ed. E. C. F. Bird (Dordrecht: Springer), 193–197. doi: 10.1007/978-1-4020-8639-7_29

Dahdouh-Guebas, F., Hettiarachchi, S., Seen, D. L., Batelaan, O., Sooriyarachchi, S., Jayatissa, L. P., et al. (2005). Transitions in ancient inland freshwater resource management in Sri Lanka affect biota and human populations in and around coastal lagoons. *Curr. Biol.* 15, 579–586. doi: 10.1016/j.cub.2005.01.053

Fatoyinbo, T. E., and Simard, M. (2013). Height and biomass of mangroves in Africa from ICESat/GLAS and SRTM. *Int. J. Remote Sens.* 34, 668–681. doi: 10.1080/01431161.2012.712224

Fromard, F., Puig, H., Mougin, E., Marty, G., Betoulle, J.-L., Cadamuro, L., et al. (1998). Structure, above-ground biomass and dynamics of mangrove ecosystems: new data from French Guiana. *Oecologia* 115, 39–53. doi: 10.1007/s004420050489

Giri, C., Ochieng, E., Tieszen, L. L., Zhu, Z., Singh, A., Loveland, T., et al. (2011). Status and distribution of mangrove forests of the world using earth observation satellite data. *Global Ecol Biogeogr.* 20, 154–159. doi: 10.1111/j.1466-8238.2010.00584.x

Hamilton, S. E., and Friess, D. (2018). Global carbon stocks and potential emissions due to mangrove deforestation from 2000 to 2012. *Nat. Clim. Change* 8, 240–244. doi: 10.1038/s41558-018-0090-4

Hamilton, S. E., Lovette, J. P., Borbor-Cordova, M. J., and Millones, M. (2017). The carbon holdings of Northern Ecuador's Mangrove Forests. *Ann. Am. Assoc. Geogr.* 107, 54–71. doi: 10.1080/24694452.2016.1226160

Hutchison, J., Manica, A., Swetnam, R., Balmford, A., and Spalding, M. (2014). Predicting global patterns in mangrove forest biomass. *Conserv. Lett.* 7, 233–240. doi: 10.1111/conl.12060

Kauffman, J. B., Adame, M. F., Arifanti, V. B., Schile-Beers, L. M., Bernardino, A. F., Bhomia, R., et al. (2020). Total ecosystem carbon stocks of mangroves across broad global environmental and physical gradients. *Ecol. Monogr* 90:e01405. doi: 10.1002/ecm.1405

Kauffman, J. B., Heider, C., Cole, T. G., Dwire, K. A., and Donato, D. C. (2011). Ecosystem carbon stocks of Micronesian mangrove forests. *Wetlands* 31, 343–352. doi: 10.1007/s13157-011-0148-9

Lagomasino, D., Fatoyinbo, T., Lee, S., Feliciano, E., Trettin, C., Shapiro, A., et al. (2019). Measuring mangrove carbon loss and gain in deltas. *Environ. Res. Lett.* 14:025002. doi: 10.1088/1748-9326/aaf0de

Lagomasino, D., Fatoyinbo, T., Lee, S., Feliciano, E., Trettin, C., and Simard, M. (2016). A comparison of mangrove canopy height using multiple independent measurements from land. *Air, and Space. Remote Sens.* 8:327. doi: 10.3390/rs8040327

Larjavaara, M., and Muller-Landau, H. C. (2013). Measuring tree height: a quantitative comparison of two common field methods in a moist tropical forest. *Methods Ecol. Evol.* 4, 793–801. doi: 10.1111/2041-210x.12071

Lee, S. K., and Fatoyinbo, T. E. (2015). TanDEM-X Pol-InSAR inversion for mangrove canopy height estimation. *IEEE J. Sel. Top. Appl. Earth Obs. Remote Sens.* 8, 3608–3618. doi: 10.1109/jstars.2015.2431646

Li, Z., Zan, Q., Yang, Q., Zhu, D., Chen, Y., and Yu, S. (2019). Remote estimation of mangrove aboveground carbon stock at the species level using a low-cost unmanned aerial vehicle system. *Remote Sens.* 11:1018. doi: 10.3390/rs11091018

Lucas, R., Van De Kerchove, R., Otero, V., Lagomasino, D., Fatoyinbo, L., Omar, H., et al. (2020). Structural characterisation of mangrove forests achieved through combining multiple sources of remote sensing data. *Remote Sens. Environ.* 237:111543. doi: 10.1016/j.rse.2019.111543

Martínez, J. O., Gonzalez, J. L., Pilkey, O. H., and Neal, W. J. (1995). Tropical barrier islands of Colombia's Pacific coast. *J. Coast. Res.* 11, 432–453.

Medina, E., Cuevas, E., Popp, M., and Lugo, A. E. (1990). Soil salinity, sun exposure, and growth of Acrostichum aureum, the mangrove fern. *Bot. Gaz.* 151, 41–49. doi: 10.1086/337803

Mejía-Rentería, J. C., Castellanos-Galindo, G. A., Cantera-Kintz, J. R., and Hamilton, S. E. (2018). A comparison of Colombian Pacific mangrove extent estimations: implications for the conservation of a unique Neotropical tidal forest. *Estuar. Coast. Shelf Sci.* 212, 233–240. doi: 10.1016/j.ecss.2018.07.020

Navarro, A., Young, M., Allan, B., Carnell, P., and Macreadie, P. (2020). The application of Unmanned Aerial Vehicles (UAVs) to estimate above-ground biomass of mangrove ecosystems. *Remote Sens. Environ.* 242:111747. doi: 10.1016/j.rse.2020.111747

Oslender, U. (2016). *The geographies of social movements: Afro-Colombian mobilization and the aquatic space.* Durham, NC: Duke University Press.

Otero, V., Van De Kerchove, R., Satyanarayana, B., Martínez-Espinosa, C., Bin Fisol, M. A., Bin Ibrahim, M. A., et al. (2018). Managing mangrove forests from the sky: forest inventory using field data and Unmanned Aerial Vehicle (UAV) imagery in the Matang Mangrove Forest Reserve, peninsular Malaysia. *For. Ecol. Manag.* 411, 35–45. doi: 10.1016/j.foreco.2017.12.049

Pettorelli, N., Wegmann, M., Skidmore, A., Mücher, S., Dawson, T. P., Fernandez, M., et al. (2016). Framing the concept of satellite remote sensing essential biodiversity variables: challenges and future directions. *Remote Sens. Ecol. Conserv.* 2, 122–131. doi: 10.1002/rse2.15

Restrepo, J. D., and Cantera, J. R. (2013). Discharge diversion in the Patia River delta, the Colombian Pacific: geomorphic and ecological consequences for mangrove ecosystems. *J. South Am. Earth Sci.* 46, 183–198. doi: 10.1016/j.jsames.2011.04.006

Restrepo, J. D., and Kjerfve, B. (2004). "The Pacific and Caribbean Rivers of Colombia: water discharge, sediment transport and dissolved loads," in *Environmental Geochemistry in Tropical and Subtropical Environments*, eds L. Lacerda, R. Santelli, E. Duursma, and J. Abrao (Berlin: Springer Verlag), 169–187. doi: 10.1007/978-3-662-07060-4_14

Rovai, A. S., Riul, P., Twilley, R. R., Castaneda-Moya, E., Rivera-Monroy, V. H., Williams, A. A., et al. (2016). Scaling mangrove aboveground biomass from site-level to continental-scale. *Glob. Ecol. Biogeogr.* 25, 286–298. doi: 10.1111/geb.12409

Rovai, A. S., Twilley, R. R., Castañeda-Moya, E., Midway, S. R., Friess, D. A., Trettin, C. C., et al. (2021). Macroecological patterns of forest structure and allometric scaling in mangrove forests. *Global Ecol. Biogeogr.* 30, 1000–1013. doi: 10.1111/geb.13268

Rovai, A. S., Twilley, R. R., Castaneda-Moya, E., Riul, P., Cifuentes-Jara, M., Manrow-Villalobos, M., et al. (2018). Global controls on carbon storage in mangrove soils. *Nat. Clim. Change* 8:534. doi: 10.1038/s41558-018-0162-5

Saliu, I. S., Satyanarayana, B., Fisol, M. A. B., Wolswijk, G., Decannière, C., Lucas, R., et al. (2021). An accuracy analysis of mangrove tree height mensuration using forestry techniques, hypsometers and UAVs. *Estuar. Coast. Shelf Sci.* 248:106971. doi: 10.1016/j.ecss.2020.106971

Scharstein, D., and Szeliski, R. (2002). A taxonomy and evaluation of dense two-frame stereo correspondence algorithms. *Int. J. Comput. Vision* 47, 7–42.

Seitz, S., Curless, B., Diebel, J., Scharstein, D., and Szeliski, R. (2006). *A comparison and evaluation of multi-view stereo reconstruction algorithms. In: Proc CVPR '06 I.E. Computer Society Conf Computer Vision and Pattern Recognition*, Vol. 1. Washington, DC: IEEE Computer Society, 519–526.

Shapiro, A. C., Trettin, C. C., Küchly, H., Alavinapanah, S., and Bandeira, S. (2015). The mangroves of the Zambezi delta: increase in extent observed via satellite from 1994 to 2013. *Remote Sens.* 7, 16504–16518. doi: 10.3390/rs71215838

Simard, M., Fatoyinbo, L., Smetanka, C., Rivera-Monroy, V. H., Castañeda-Moya, E., Thomas, N., et al. (2019). Mangrove canopy height globally related to precipitation, temperature and cyclone frequency. *Nat. Geosci.* 12, 40–45. doi: 10.1038/s41561-018-0279-1

Simard, M., Rivera-Monroy, V. H., Mancera-Pineda, J. E., Castañeda-Moya, E., and Twilley, R. R. (2008). A systematic method for 3d mapping of mangrove forests based on shuttle radar topography mission elevation data, ICEsat/GLAS waveforms and field data: application to Ciénaga Grande de Santa Marta, Colombia. *Remote Sens. Environ.* 112, 2131–2144. doi: 10.1016/j.rse.2007.10.012

Spalding, M. D., Fox, H. E., Allen, G. R., Davidson, N., Ferdaña, Z. A., Finlayson, M., et al. (2007). Marine ecoregions of the world: a bioregionalization of coastal and shelf areas. *Bioscience* 57:573. doi: 10.1641/B570707

Trettin, C. C., Dai, Z., Tang, W., Lagomasino, D., Thomas, N., Lee, S. K., et al. (2021). Mangrove carbon stocks in Pongara National Park, Gabon. *Estuar. Coast. Shelf Sci* 259:107432. doi: 10.1016/j.ecss.2021.107432

Ullman, S. (1979). The interpretation of structure from motion. *Proc. R. Soc. Lond. B Biol. Sci.* 203, 405–426.

West, R. C. (1956). Mangrove swamps of the Pacific coast of Colombia. *Ann. Assoc. Am. Geogr.* 46, 98–121. doi: 10.1111/j.1467-8306.1956.tb01498.x

Westing, A. H. (1983). The environmental aftermath of warfare in Viet Nam. *Nat. Resour. J.* 23, 365–389.

Westoby, M. J., Brasington, J., Glasser, N. F., Hambrey, M. J., and Reynolds, J. M. (2012). 'Structure-from-Motion' photogrammetry: a low-cost, effective tool for geoscience applications. *Geomorphology* 179, 300–314. doi: 10.1016/j.geomorph.2012.08.021

Worthington, T. A., Andradi-Brown, D. A., Bhargava, R., Buelow, C., Bunting, P., Duncan, C., et al. (2020). Harnessing big data to support the conservation and rehabilitation of mangrove forests globally. *One Earth* 2, 429–443. doi: 10.1016/j.oneear.2020.04.018

Zanne, A. E., Lopez-Gonzalez, G., Coomes, D. A., Ilic, J., Jansen, S., Lewis, S. L., et al. (2009). *Global Wood Density Database. Dryad. Identifier.* Available online at: http://hdl.handle.net/10255/dryad.235 (accessed March 2, 2021).

Zeng, Y., Friess, D. A., Sarira, T. V., Siman, K., and Koh, L. P. (2021). Global potential and limits of mangrove blue carbon for climate change mitigation. *Curr. Biol* 31, 1737–1743.e3.